

Thermal Management of the ALPIDE Space Module for Particle Tracking



Roadmap towards a collaborative multi-physics simulation workflow for **defense applications**

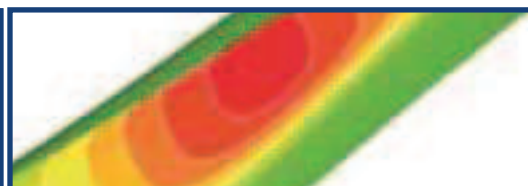
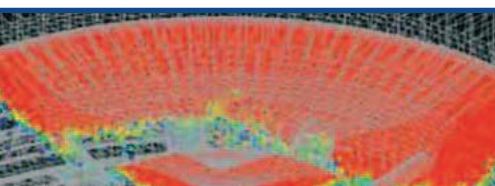
New MPS-based method to design and analyse the **cooling systems** of engine pistons is **faster and more accurate**

The multiscale and **optimization analysis** of a **lattice structure** produced via additive manufacturing

Virtual Reality Application in a **Nuclear Accelerator Facility**

Analysis of **flow characteristics** in an **urban area** using CFD

What future does **digital transformation** predict?





Medical Digital Twins used to help predict pathology evolution and the effect of surgical corrections in cardiovascular patients

Reduced-order model and mesh morphing techniques facilitate the generation of results in near-real-time without High Performance Computers

Nowadays in silico analysis tools in the bio-medical field are moving from the research context to patient-specific treatment and prevention. Hemo-dynamics is receiving great attention, and accurate Computational Fluid Dynamics (CFD) modelling can be adopted to produce a digital medical twin capable of reliably predicting the pathology evolution, and the effect of surgical corrections. The availability of in silico digital twins based on computer-assisted engineering (CAE) simulations is one of the key enablers; the parametric shape of vessels and reduced-order models (ROM) are promising solutions. The ROM approach usually requires the use of high-performance computing (HPC), but it can also be executed almost in real time and outside the standard CAE tools as well. This paper demonstrates the concept using the new ROM Builder available in ANSYS 19.1. We developed a pipeline for an aortic aneurysm to study the effect of a bulge-shaped progression on the flow field. First, a patient-specific geometry was reconstructed, then a CFD model was created with a bulge shape that was parameterised using a radial basis function (RBF) mesh morphing technique. Finally, a ROM was suitably built up by conducting CFD simulations. We provide examples of fast evaluations that were achieved off-line by using the ROM results.

Tackling cardiovascular disease, the world's leading cause of death Cardiovascular disease (CVD) is the main cause of death in the world, resulting in 17.9 million deaths (32.1%) in 2015 alone [1]. It is estimated that up to 90% of these casualties could be predicted and prevented [2]. In silico analysis can help in this regard, improving these figures by analysing patient-specific tailored systems for prevention. The evolution and growing availability of computational power has extended this

concept by enabling the use of high-fidelity CAE simulations and the development of medical digital twins that provide a safe environment in which to predict the pathology evolution and to explore the impact of potential surgical corrections. For CVD pathologies, the hemo-dynamics of the vessels can be thoroughly examined by using high-fidelity CFD techniques and tools. The large quantity of degrees of freedom inherent in a real clinical case, however, make this approach computationally expensive and less suitable for testing patient-specific cases virtually and in real time. While several methodologies, such as the use of stochastic approaches for geometrical variations, material properties and uncertainty quantification [3][4][5], have been developed to overcome this problem, as can be seen in the literature, none of them can cope with the full field of variables of interest to provide quantitative output in real time. It is here that ROMs are emerging as a viable technology that can provide complex, multi-degree-of-freedom, full-scale solutions while drastically reducing the overall computing cost.

The use of ROM systems is well-known and has received significant attention in the last decade, but this use has mainly been limited to classical mechanics [6] and dynamics [7]; their implementation in the field of biomechanics is very recent and is limited to only a few works [8]. Furthermore, the ROM's ability to investigate the effect of an enormous number of parameters in real time can be synergistically combined with mesh-morphing techniques that can provide a vast number of geometrical variations. Radial basis functions [9] have been demonstrated to be powerful morphing tools in several fields, including the medical one [10]. In this paper, a workflow envisioning the use of the ROM implementation

available in ANSYS 19.1 together with the commercial morpher RBF Morph is proposed and applied to the investigation of the hemodynamic fields for a wide set of ascending thoracic aneurysmatic aortic (ATAA) morphologies. The following section briefly gives the background of ROM and RBF. The proposed workflow is then introduced and demonstrated for execution on an ATAA test case.

A brief background of reduced-order model (ROM) and radial basis function (RBF)

ROM: Reduced-Order Model

Model Reduction is a technique that allows cost-efficient evaluation of systems with a large degree-of-freedom (DOF) by reducing the number of variables involved in the problem. This simplification, while preserving the essential characteristics of the system to enable an accurate and efficient representation, makes real-time control over the parameters of the problem feasible. ROMs have been successfully applied over the years to controls [11], fluid dynamics, structural dynamics, thermal analysis, multi-physics [12], medical [13] and optimization problems [14]. Several techniques to obtain a ROM representation have been explored and are available to the scientific community in the literature. The technique employed in this paper is based on Proper Order Decomposition (POD) which is implemented as commercial software in ANSYS Workbench 19.1 [15]. A typical workflow that includes the use of ROM, shown in figure 1, is composed of two main tasks that are typically referred to as creation and consumption. The first task -- the training of the ROM using a simulation software and extracting the most important modes using a POD technique -- deals with all the processes necessary to generate and extract the information from the full DOF system. The latter task uses these extracted modes to produce a reduced order system in real time. This can be accomplished either by using the ANSYS ROM viewer, a standalone software designated to ROM consumption, or by importing the reduced system into ANSYS Fluent.

Since the reduced system is a direct consequence of the variation in the input parameters and of the generation of several Design Points (DPs), the ROM environment implemented by ANSYS is designed to be strongly entwined with the Response Surface (RS) concept. Indeed, the generation of the training data is produced by evaluating a given number of DPs, called snapshots, at full scale. The higher the number of snapshots, the more faithful the reduced order model, which then captures all the nuances of the system



Fig. 1 - ANSYS ROM usage workflow

produced by a parameter variation. The quality of the reduced model is also influenced by the number of modes employed for its discretization. ANSYS Workbench allows the result of the ROM creation task to be saved as a standalone file that includes the reduced system as well as the numerical grid of the problem. When necessary, this file can then be imported into the consumption task by exploiting the standalone ANSYS ROM viewer, or it can be loaded into ANSYS Fluent as an alternative to the *.cas and *.dat files.

RBF: Radial basis function

From a mathematical point of view, the solution of an RBF problem consists of calculating the coefficients of a linear system of order equal to the number of source points (De Boer et al., 2007), by means of which the displacement of an arbitrary mesh's node (target) can be expressed, and then imposed, as the summation of the radial contribution of each controlled node (source). In this way, mesh smoothing can be rapidly applied by maintaining the mesh topology expressed in terms of the total number and type of elements.

In particular, the RBF Morph tool uses the RBF interpolant s composed of a radial function that contains the RBF φ and a multivariate polynomial corrector vector h of the order $m-1$, where m is said to be the order of φ , introduced with the aim of assuring the uniqueness of the RBF solution and its compatibility for rigid motion. Specifically, if N is the total number of source points, the formulation of the RBF interpolant is

$$s(\mathbf{x}) = \sum_{i=1}^N \gamma_i \varphi(\|\mathbf{x} - \mathbf{x}_{k_i}\|) + h(\mathbf{x}) \quad (1)$$

where \mathbf{x} is the vector identifying the position of a generic node belonging to the surface, and/or volume mesh \mathbf{x}_{k_i} is the i th source node position vector; $\|\cdot\|$ is the Euclidean norm.

The fitting RBF solution exists in the case that the RBF coefficients vector γ_i and the weights of the polynomial corrector vector β_i can be found such that the interpolant function, at the source points, possesses the specified (known) values of displacement g_i , whilst the polynomial terms give a null contribution. In other words, the following relations

$$s(\mathbf{x}_{k_i}) = g_i \quad 1 \leq i \leq N \quad (2)$$

$$\sum_{i=1}^N \gamma_i q(\mathbf{x}_{k_i}) = 0 \quad (3)$$

are simultaneously verified for all polynomials q with a degree less than or equal to that of polynomial h (Beckert and Wendland, 2001). The minimal degree of polynomial h is dependent on the choice of RBF type. It can be demonstrated that a unique RBF interpolant exists if the RBF is conditionally positive definite (Van Zuijlen et al., 2007). In the case that this latter condition is established, and if the order is less than or equal to 2 (Jin et al., 2001), a linear polynomial applies

$$h(\mathbf{x}) = \beta_1 + \beta_2 x + \beta_3 y + \beta_4 z \quad (4)$$

enabling the exact recovery of the rigid body translations.

In the event such assumptions are verified, the interpolant has the form

$$s(\mathbf{x}) = \sum_{i=1}^N \gamma_i \varphi(\|\mathbf{x} - \mathbf{x}_{k_i}\|) + \beta_1 + \beta_2 x + \beta_3 y + \beta_4 z \quad (5)$$

and the values for γ_i and β_j can be obtained by solving the system

$$\begin{pmatrix} \mathbf{U} & \mathbf{P} \\ \mathbf{P}^T & \mathbf{0} \end{pmatrix} \begin{pmatrix} \boldsymbol{\gamma} \\ \boldsymbol{\beta} \end{pmatrix} = \begin{pmatrix} \mathbf{g} \\ \mathbf{0} \end{pmatrix} \quad (6)$$

where \mathbf{U} is the interpolation matrix whose elements are derived by calculating all the radial interactions between the source points, as follows

$$U_{ij} = \varphi(\|\mathbf{x}_{k_i} - \mathbf{x}_{k_j}\|) \quad 1 \leq i \leq N, \quad 1 \leq j \leq N \quad (7)$$

and \mathbf{P} is a constraint matrix that arises from balancing the

$$\mathbf{P} = \begin{pmatrix} 1 & x_{k_1} & y_{k_1} & z_{k_1} \\ 1 & x_{k_2} & y_{k_2} & z_{k_2} \\ \vdots & \vdots & \vdots & \vdots \\ 1 & x_{k_N} & y_{k_N} & z_{k_N} \end{pmatrix} \quad (8)$$

assuming that the source points are not contained in the same plane (otherwise the interpolation matrix would be singular).

Radial Basis Functions (RBF) with global support	$\varphi(r)$
Spline type (Rn)	$r^n, n \text{ odd}$
Thin plate spline (TPSn)	$r^n \log(r), n \text{ even}$
Multiquadric (MQ)	$\sqrt{1+r^2}$
Inverse multiquadric (IMQ)	$\frac{1}{\sqrt{1+r^2}}$
Inverse quadratic (IQ)	$\frac{1}{1+r^2}$
Gaussian (GS)	e^{-r^2}
Radial Basis Functions (RBF) with compact support	$\varphi(r) = f(\xi), \xi \leq 1, \xi = \frac{r}{R_{sup}}$
Wendland C0 (C0)	$(1-\xi)^2$
Wendland C2 (C2)	$(1-\xi)^2(4\xi+1)$
Wendland C4 (C4)	$(1-\xi)^2\left(\frac{35}{3}\xi^2+6\xi+1\right)$

Table 1: Typical RBF

As has been described, by satisfying the displacement field prescribed at the source points, RBF Morph smoothes the mesh nodes by using the following formulation of the interpolant

$$\begin{cases} s_x(\mathbf{x}) = \sum_{i=1}^N \gamma_i^x \varphi(\|\mathbf{x} - \mathbf{x}_{k_i}\|) + \beta_1^x + \beta_2^x x + \beta_3^x y + \beta_4^x z \\ s_y(\mathbf{x}) = \sum_{i=1}^N \gamma_i^y \varphi(\|\mathbf{x} - \mathbf{x}_{k_i}\|) + \beta_1^y + \beta_2^y x + \beta_3^y y + \beta_4^y z \\ s_z(\mathbf{x}) = \sum_{i=1}^N \gamma_i^z \varphi(\|\mathbf{x} - \mathbf{x}_{k_i}\|) + \beta_1^z + \beta_2^z x + \beta_3^z y + \beta_4^z z. \end{cases} \quad (9)$$

RBF enables great flexibility in acting on the radial functions, which can be compactly or globally supported. The common options are summarized in Table 1. RBF Morph allows four radial functions.

The distance function (global support and bi-harmonic in 3D) is used by default and performs very well in volume morphing, as it allows one to obtain very high quality and it is accelerated so that it can handle RBF problems of beyond 1 million centres (source points). Wendland functions (C0, C2 and C4) are available for

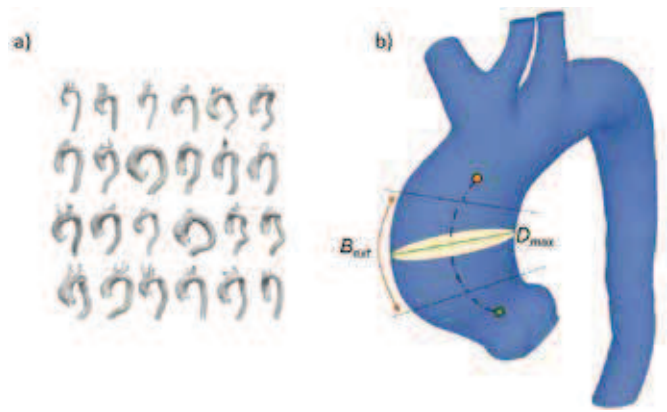


Fig. 2 - Statistical aneurysmatic aorta

surface sculpting since the high level of continuity can be used to check a surface using just a few control points.

Application description

The application selected to describe the proposed workflow is an ascending aorta aneurysm. In the following sections, the ROM and RBF set-ups are provided in detail.

CFD-model generation

The geometry considered, and its shape variations, are the result of processing the data pertaining to an aneurysmatic aorta SSGA, which has been defined according to the procedure described in Capellini et al. [16]. The 3D-model was obtained from the statistical analysis of the aortic morphological shapes of 45 aneurysmatic patients (Fig.2a) whose CT datasets were retrospectively segmented and elaborated using VMTK software and Python custom scripts. The

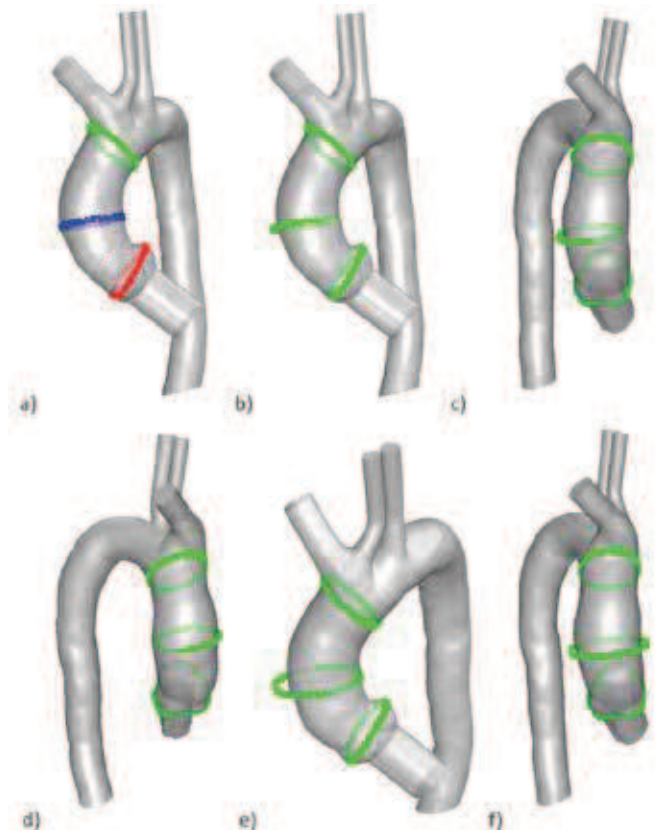


Fig. 3 - RBF set-up. Source points and their displacement

SSGA model was parameterized to create a CFD model that could cope with many ascending aneurysmatic aortic configurations through shape deformations. Three of the parameters evaluated in the previous statistical analysis work were considered to follow the bulge variations: the maximum diameter of the aneurysm (D_{max}), the tortuosity value (T) of the centreline of the ascending portion of aorta, and the bulge extension (B_{ext}). These parameters were assumed to vary at specific intervals that were extracted from the results of the statistical analysis reported in Capellini et al. [16]. We considered a range of average values \pm standard deviations for each parameter ($D_{max} = [45.69-55.95 \text{ mm}]$, $T = [0.0776-0.1484]$, $B_{ext} = [17.93-41.69 \text{ mm}]$). Figure 2(b) depicts the SSGA model including the ascending centreline, the D_{max} and the B_{ext} .

RBF set-up

The mesh morphing action was accomplished using the commercial morpher RBF Morph. A set of source points on the ascending thoracic aortic region was selected to generate five shape-variations representative of the statistical geometry explained in the previous section. Figure 3 shows the RBF set-up. Three sets of RBF points were generated, as shown in Figure 3a, by maintaining fixed the extremal sets (green and red in the picture) in order to circumscribe the morphing action. The central set was translated into the plane over which the points were defined (Figure 3b, 3c and 3d), and was scaled over the same plane along the principal directions (Figure 3e and 3f). This set of five shape-modifications was chosen to generate the representative variations shown in Figure 2a. The time required to morph the 1.5 million-element tetrahedral CFD mesh for each DP was 43s using an i7 laptop with 16 GB of RAM.

ROM set-up

As previously described, the ROM extraction process requires the evaluation of several high-fidelity snapshots. This problem

considered five shape parameters. Consequently, a number of snapshots had to be chosen to capture all the important characteristics of the system: 40 snapshots, selected via the Kriging method, were taken to seed the DP in the parameter space. The first five orthogonal modes were extracted with the POD to obtain a model that was reduced to 5 DOF. It was decided to only extract 5 modes because the error that would have been introduced by using 10 modes was below 1%, as shown in Figure 4, where the pressure results obtained using 5 modes (top row) are compared to the ones gained employing 10 modes (bottom row). This comparison was made by varying the flow according to three levels of accretion of the aneurism.

Results

To assess the quality of the proposed methodology, the results obtained using ROM were compared to those achieved using plain CFD evaluations. Figure 5 shows the pressure contours and streamlines obtained through ROM for the three degrees of accretion of the aneurism (in the first row), while the ones calculated using a full CFD computation are shown in the last row. The maximum discrepancy between the two methodologies is in the order of 2.5%. Although this error could be further decreased by enriching the number of snapshots and employing a higher number of orthogonal modes, it was judged to be acceptable because each new ROM evaluation could be visualised in almost real-time whereas the CFD calculations required about half an hour.

Conclusions

The activities described in this paper deal with a critical aspect of digital twins: the need to gain computational results in real time. Since high-fidelity CFD simulations, which have already proven to be useful in predicting the growth and evolution of CVD pathologies, require a lot of computational effort, a methodology to overcome this problem was proposed. ROM has proven to be very efficient in reducing the computing costs for complex multi-degree-of-freedom models (like CFD models). On the other hand, RBF mesh morphing has proven to be highly efficient in generating different shapes for numerical models, thus reducing the time required to generate new ones. The proposed methodology envisages the synergetic use of ROM and RBF mesh morphing to generate a new shape for the CFD model including its numerical results from a discrete set of shape configurations. The proposed methodology was developed in the ANSYS® Workbench™ 19.1 environment by exploiting the ROM functionalities provided by this release of the software together with the RBF-Morph™ Fluent® add-on. The complete workflow was tested in a CFD study of an ascending thoracic aortic aneurysm. The results obtained with the proposed approach were then compared to regular CFD evaluations, which required the full CFD solution of the new shapes of the aneurism. A good agreement in terms of the monitored variables was finally obtained. The successful application of the proposed methodology led to the conclusion

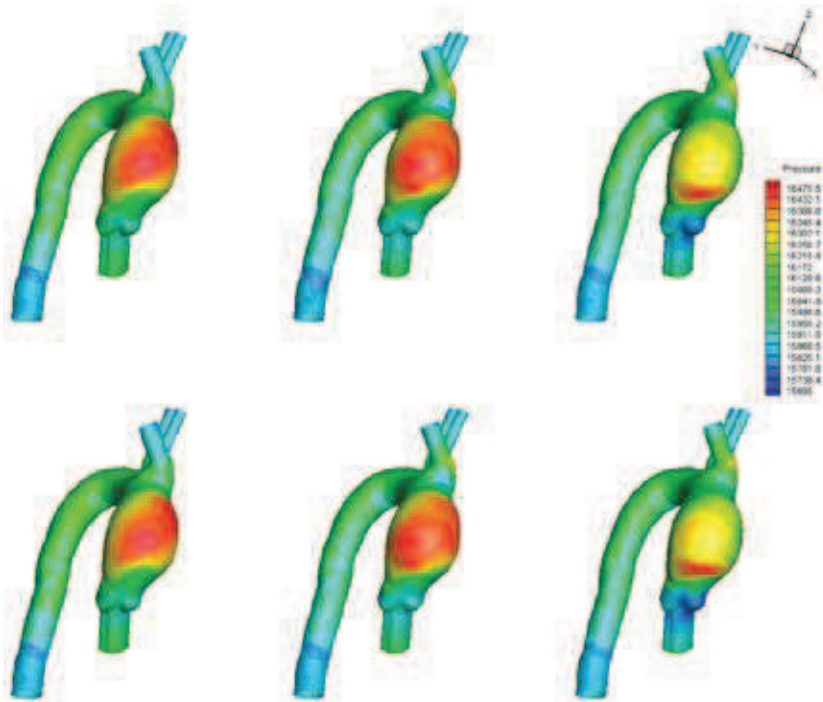


Fig. 4 - ROM results with 5 modes (top) and 10 modes (bottom)

that it can be successfully exploited to assist in the generation and fruition of digital twins in medical applications.

References

- [1] GBD 2015 Mortality and Causes of Death, Collaborators. (8 October 2016). "Global, regional, and national life expectancy, all-cause mortality, and cause-specific mortality for 249 causes of death, 1980-2015: a systematic analysis for the Global Burden of Disease Study 2015". *Lancet*. 388 (10053): 1459–1544. doi:10.1016/S0140-6736(16)31012-1.
- [2] McGill HC, McMahan CA, Gidding SS (March 2008). "Preventing heart disease in the 21st century: implications of the Pathobiological Determinants of Atherosclerosis in Youth (PDAY) study". *Circulation*. 117 (9): 1216–27. doi:10.1161/CIRCULATIONAHA.107.717033.
- [3] Celi, S., and Berti, S., 2012. "Biomechanics and FE modelling of aneurysm: Review and advances in computational models". In *Aneurysm*. InTech.
- [4] Celi, S., and Berti, S., 2013. "Three-dimensional sensitivity assessment of thoracic aortic aneurysm wall stress: a probabilistic finite-element study". *European Journal of Cardio-Thoracic Surgery*, 45(3), pp. 467–475
- [5] Boccadifuoco, A., Mariotti, A., Celi, S., Martini, N., and Salvetti, M., 2018. "Impact of uncertainties in outflow boundary conditions on the predictions of hemodynamic simulations of ascending thoracic aneurysms". *Computers & Fluids*, 165, pp. 96–115
- [6] Alonso, D., Velazquez, A., and J.M., V., 2009. "A method to generate computationally efficient reduced order models". *Comput. Methods Appl. Mech. Engrg*, 198(-), pp. 2683–2691
- [7] Gennaretti, M., and Mastroddi, F., 2004. "Study of Reduced-Order Models for Gust-Response Analysis of Flexible Fixed Wings". *Journal of Aircraft*, 41(2), pp. 304–313.
- [8] Niroomandi, S., Alfaro, I., Gonzlez, D., Cueto, E., and Chinesta, F. "Real-time simulation of surgery by reduced-order modeling and x-fem techniques". *International Journal for Numerical Methods in Biomedical Engineering*, 28(5), pp. 574–588.
- [9] Buhmann, M. D., 2000. "Radial basis functions". *Acta Numerica* 2000, 9(247), Jan, pp. 1–38
- [10] Biancolini, M., Ponzini, R., Antiga, L., and Morbiducci, U., 2012. "A new workflow for patient specific image-based hemodynamics: parametric study of the carotid bifurcation". *Comput Model Objects Represented Images III: Fundam Methods Appl*.
- [11] Bailey, E. A., Dutton, A. W., Mattingly, M., Devasia, S., and Roemer, R. B., 1998. "A comparison of reduced-order modelling techniques for application in hyperthermia control and estimation". *International Journal of Hyperthermia*, 14(2), pp. 135–156
- [12] Gennaretti, M., and Mastroddi, F., 2004. "Study of Reduced-Order Models for Gust-Response Analysis of Flexible Fixed Wings". *Journal of Aircraft*, 41(2), pp. 304–313
- [13] Ballarin, F., Faggiano, E., Ippolito, S., Manzoni, A., Quarteroni, A., Rozza, G., and Scrofani, R., 2016. "Fast simulations of patient-specific haemodynamics of coronary artery bypass grafts based on a POD-Galerkin method and a vascular shape parametrization". *Journal of Computational Physics*, 315, pp. 609–628
- [14] Karpel, M., 1999. "Reduced-Order Models for Integrated Aeroservoelastic Optimization". *Journal of Aircraft*, 36(1), pp. 146–155.
- [15] Chaturantabut, S., and Sorensen, D. C., 2012. "A State Space Error Estimate for POD-DEIM Nonlinear Model Reduction". *SIAM Journal on Numerical Analysis*, 50(1), pp. 46–63
- [16] Capellini, K., Vignali, E., Costa, E., Gasparotti, E., Biancolini, M., Landini, L., Positano, V., and Celi, S., 2018. "Computational fluid dynamic study for ATAA hemodynamics: an integrated image-based and RBF mesh morphing approach". *Journal of Bio-mechanical Engineering*. in-press

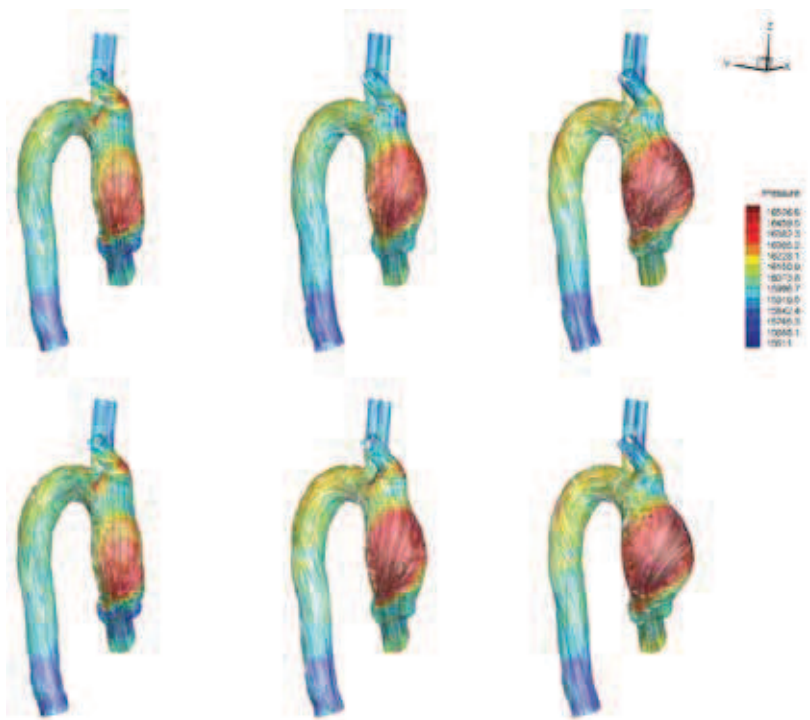


Fig. 5 - ROM results (top) compared to CFD (bottom)

*Corrado Groth, Stefano Porziani, Marco Evangelos Biancolini
University of Rome Tor Vergata's Dep. of Enterprise Engineering in Rome*

Emiliano Costa - RINA Consulting S.p.A

*Simona Celi, Katia Capellini
BioCardioLab's Bioengineering Unit at the Fondazione Toscana "G.
Monasterio"*

Michel Rochette, Valery Morgenthaler - ANSYS France

**Smart Products & IoT Session of the
International CAE Conference 2018**
proceedings2018.caeconference.com